7-23-75
25 cp. NTIS

UCRL-76491
PREPRINT
CONF-750424--5

LAWRENCE LIVERMORE LABORATORY
University of California/Livermore, California

THEORETICAL X-RAY CONVERSION EFFICIENCIES AND SPECTRA OF SINGLE ELEMENT PLANE TARGETS HEATED BY HUNDRED PICOSECOND LIGHT PULSES FROM NEODYMIUM GLASS LASERS

W. H. Grasberger
C. E. Violet
L. M. Richards

July 1975

This paper was prepared for submission to
APS Meeting, Washington D.C., April 30, 1975

MASTER

Talk Given at the APS Washington Meeting
on April 30, 1975 by W. H. Grasberger

Theoretical X-Ray Conversion Efficiencies and Spectra of Single Element Plane Targets Heated by Hundred Picosecond Light Pulses from Neodymium Glass Lasers.

W. H. Grasberger, C. E. Violet, and L. M. Richards.*

---

*Worked performed under the auspices of the Energy Research and Development Administration and the Defense Nuclear Agency.

A non-LTE rate equation computer program was recently combined with a program devised by Dr. Ray Kidder, which simulates the heating of laser-heated targets in plane geometry. The hydrodynamic program calculates the absorption of laser light, the electron and ion temperatures - allowing for electron heat conduction - and the densities each time-step and feeds these values to the rate equation program. The rate equation program gives to the hydrodynamic program for each time-step a source-sink term for each hot zone above 20 eV. representing the net emission and absorption of X-rays. Our calculations involve approximately ten "cool" and ten "hot" zones.

Each state of an ion is designated by the number of bound electrons - i - and by the shell n ($\leq$10) of the excited electron, assuming single excitation only. We assume j-j coupling, so that the sublevels of the ten shells total 100. Each shell is assumed to be in statistical equilibrium, with the line transitions occurring between subshells according to the usual selection rules. An ionic chain can have up to twelve ions at any time, with additions or substractions occurring at the ends as required. Hence, up to 120 rate equations are solved simultaneously per zone. Dr. James Scofield supplies the energy levels and f-values of each element. For example, zirconium with Z=40 has 4000 energy levels.

The physical processes involved in the rate equation solution include electron impact excitation and ionization, 3-body recombination, radiative recombination, and line emission and absorption. Continuous emission and absorption is treated by solving the equation of transfer analytically, ignoring time-retardation, for up to 200 energy points. Lines are treated by calculating a representative scale length for each line and by calculating the probability of line photons escaping without local reabsorption, using a Doppler profile.

To convert from a two-dimensional laser light distribution on the target to a one-dimensional representation we assumed a Gaussian intensity distribution and approximated our one - D intensity by multiplying ln2 by the average intensity within the diameter of the circle where half the light energy falls.

The experimental results for targets of aluminum, iron, and zirconium using a 1-5 joules, 300 ps glass laser were described by the previous speaker. Our calculations to simulate these experiments used a shorter pulse of 150 ps in order to compensate for 2-D effects which become increasingly more probably after 100 ps. A nominal light spot diameter of 100 microns was assumed, althrough the large experimental scatter suggests large variation of spot size from experiment to experiment.

The first slide (#1) shows an example of the ionic population history for the hot zones for a zirconium target heated by laser light of 5 X 10^{13} watt/cm^2. This is for ions with ten bound electrons. Zone 9 is the outermost zone.

This slide (#2) gives for a typical zone the various ionic population histories. At early times electrons are being stripped off ions with these sinusoidal set of curves. At 100 eV the zone switches from LTE to non-LTE, as indicated by the abrupt changes at 4 ps. There is a quick recovery and the ionization proceeds - at a slower rate. Recombination starts when the laser light ends.

This slide (#3) shows the ionic population history for the outermost zone. Because of the low density the ions appear to be "frozen" even after the laser light ceases.

This slide (#4) shows the electron temperatures. The peak temperature is slightly over one kilovolt. Note the fall-off at the end of the laser light.

This slide (#5) shows the continuous X-ray spectrum calculated for the zirconium target.

This slide (#6) shows the line strengths for X-rays, where our calculations ignore inner shell transitions. The group of lines here are $n = 2$ to 3 transitions, and this group are $n = 2$ to $n > 3$. Both groups of lines are produced by ions with ten or less electrons. This group of lines is produced by all ions and there are several thousand lines.

In this slide (#7) the region of 2-3 KeV produced by ions with ten electrons show only seven lines, in j-j coupling for the n = 2 to 3 transitions.

The same region is shown in the next slide (#8) showing a microdensitometer tracing obtained experimentally by Dr. Warren Meade. Six lines indicated here are due to neon-like zirconium, and were first identified by Dr. James Scofield. The seventh line is probably here but too weak to show above these satellite lines, which are probably due to inner shell excitation of ions with eleven or more electrons. A calculation at the lower intensity of 2×10^{13} watt/cm^2 was run and its line pattern is shown in the next slide (#9). Rough agreement with experiment occurs, but the first pair of lines is too weak and the last pair of lines have their relative intensities in reverse order.

The line strengths for iron for an intensity of 5×10^{13} watt/cm^2 is shown next (#10). These are K-shell lines, here are L-shell lines, and these are M and higher shell lines. The next slide (#11) shows the L-shell lines in more detail. Here are lines whose upper shell is n = 3 and here are lines with $n > 3$. Ions with ten electrons produce this set of lines and so forth up to these lines produced by ions with only four electrons. Comparing with experiment, the next slide (#12) shows lines produced by a 16 joule 3 ns laser. The fall off of lines occurs for ions with eight electrons, indicating a cooler temperature.

Since I don't have an experimental aluminum line spectrum to show, a silicon-lead target spectrum will have to suffice. The next slide (#13) was produced by a 10 joule, 100 ps glass laser. These are silicon lines due to hydrogen-like and helium-like ions. This "band" is probably due to n = 4 to 3 lines of lead. Calculations for a silicon target indicate qualitative agreement.

The experimental X-ray efficiencies discussed by the previous speaker will now be compared with calculations. This slide (#14) shows the efficiencies for iron targets. Note the calculated values with Be absorbers are somewhat high. The next slide (#15) shows efficiencies for aluminum targets. The 1/2 mil Be experiment lies below the calculation, but there is a rapid fall-off with decreasing intensity. The next slide (#16) shows the zirconium targets, and a rather large discrepancy between calculation and experiment.

By using an intensity of $1.3\text{X}10^{13}$ watt/cm^2 we obtain agreement with the aluminum experiment. Using this intensity and extrapolating the crosses in the next slide (#17) indicate the calculated values. We have now "explained" the observed efficiencies for Al, Fe, and Zr reasonably well. These higher Z cases have not yet been calculated.

To conclude: one dimensional calculations appear to be adequate for laser pulses of less than 100 ps in calculating X-ray spectra and efficiencies.

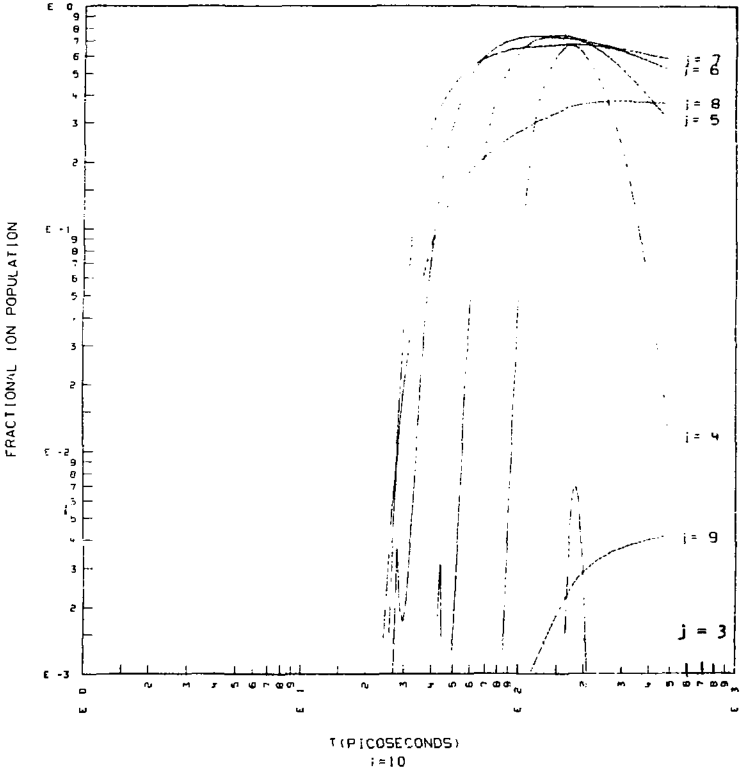
FRACTIONAL ION POPULATION
E 0
E -1
E -2
E -3
T(PICOSECONDS)
i=10
j = 7
j = 6
j = 8
j = 5
j = 4
j = 9
j = 3

Figure (1)

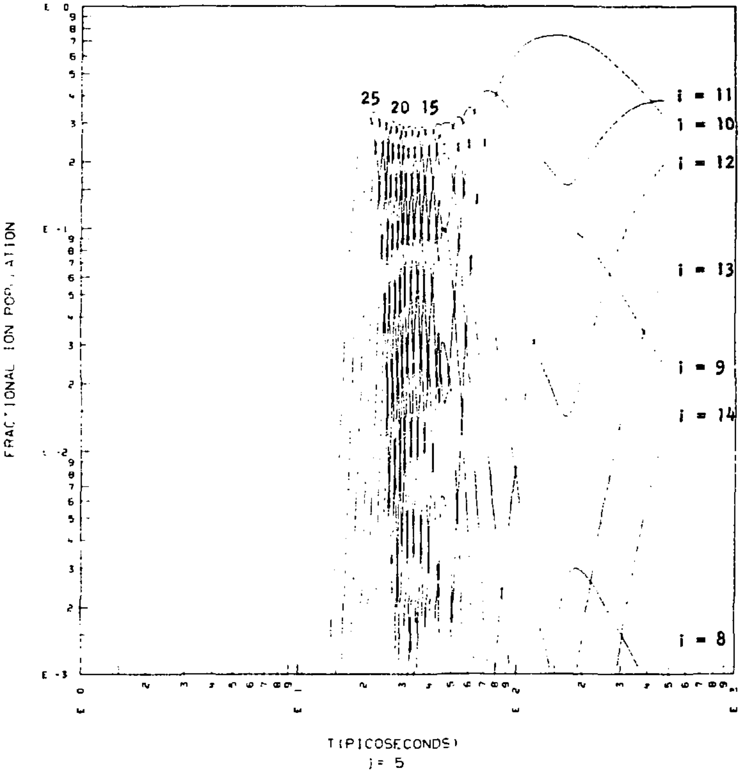
E 0
E -1
E -2
E -3
FRACTIONAL ION POPULATION
25
20
15
i = 11
i = 10
i = 12
i = 13
i = 9
i = 14
i = 8
T(PICOSECONDS)
j = 5

Figure (2)

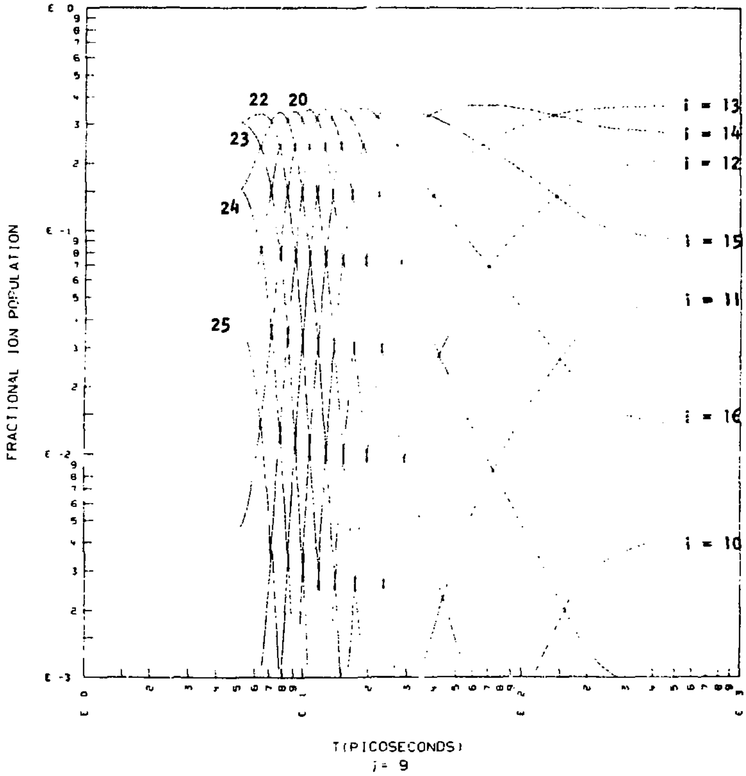
FRACTIONAL ION POPULATION
T(PICOSECONDS)
j = 9
E 0
E -1
E -2
E -3
22
20
23
24
25
i = 13
i = 14
i = 12
i = 15
i = 11
i = 16
i = 10

Figure (3)

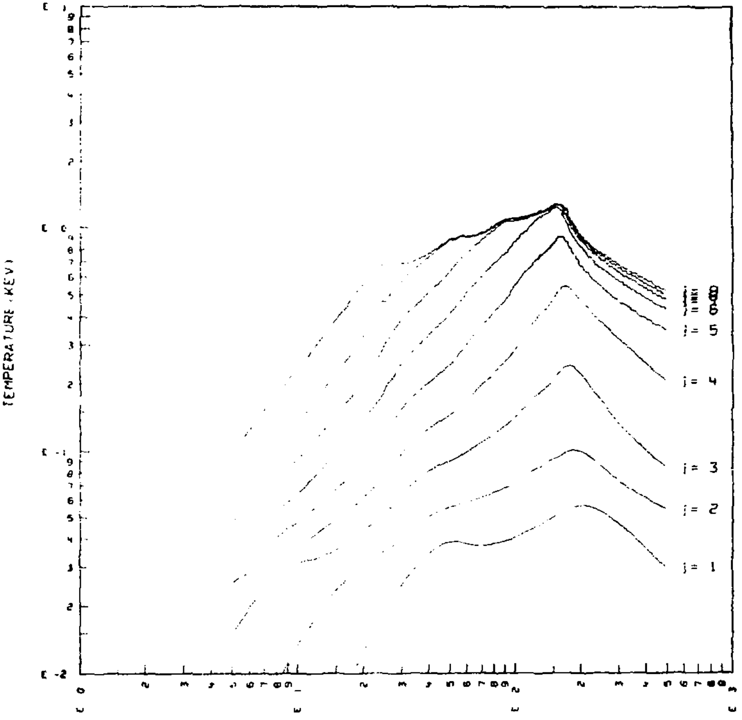

Figure (4)

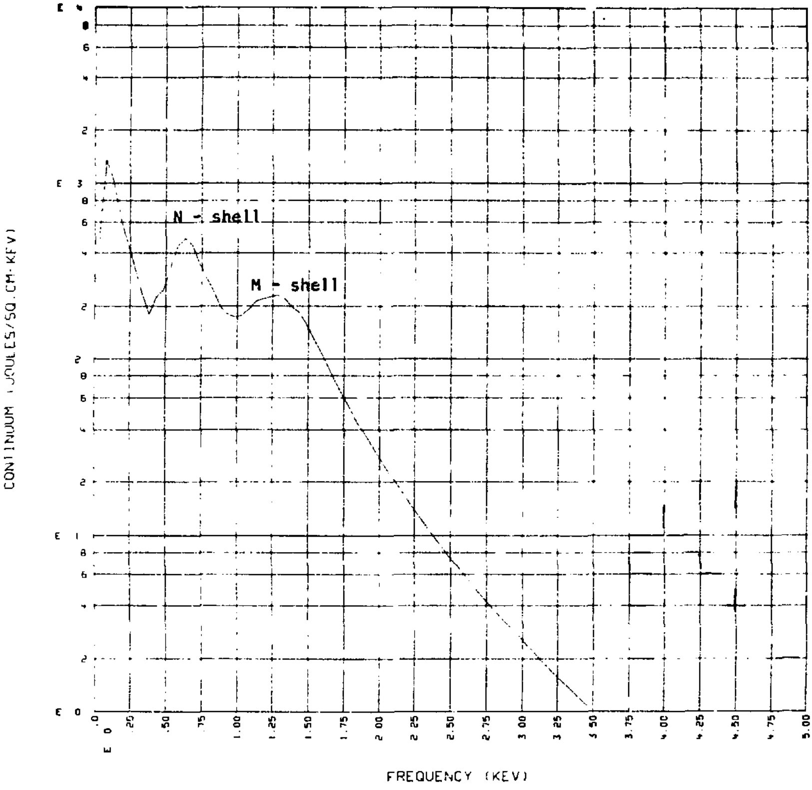

CONTINUUM (JOULES/SQ.CM.KEV)
FREQUENCY (KEV)
N - shell
M - shell
E 4
8
6
4
2
E 3
E 2
E 1
E 0
.0
.25
.50
.75
1.00
1.25
1.50
1.75
2.00
2.25
2.50
2.75
3.00
3.25
3.50
3.75
4.00
4.25
4.50
4.75
5.00

Figure (5)

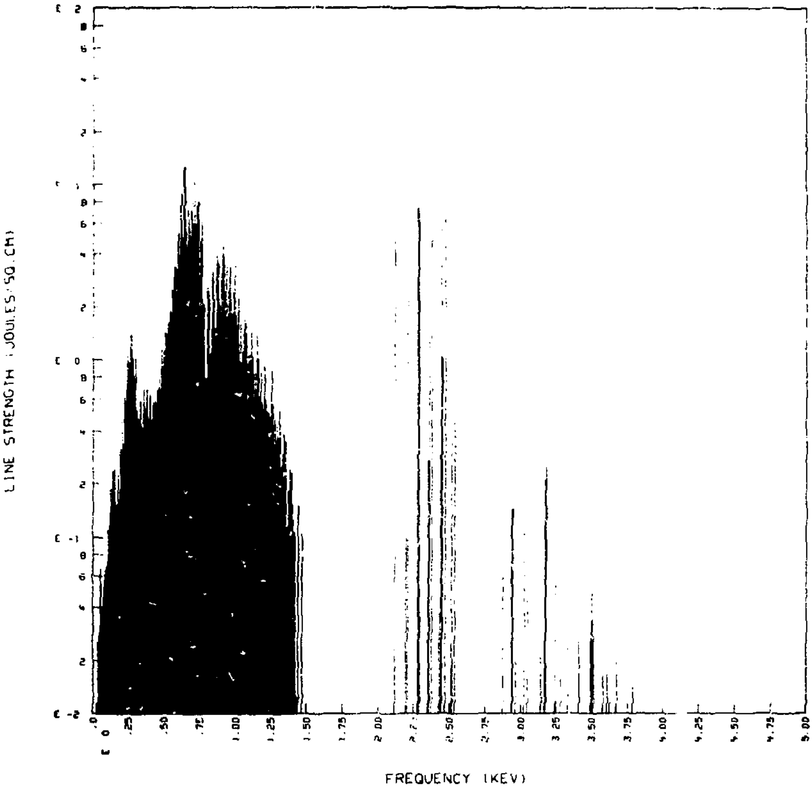
LINE STRENGTH (JOULES/SQ.CM)
E 2
8
6
4
2
E 1
8
6
4
2
E 0
8
6
4
2
E -1
8
6
4
2
E -2
.0
E 0
.25
.50
.75
1.00
1.25
1.50
1.75
2.00
2.25
2.50
2.75
3.00
3.25
3.50
3.75
4.00
4.25
4.50
4.75
5.00
FREQUENCY (KEV)

Figure (6)

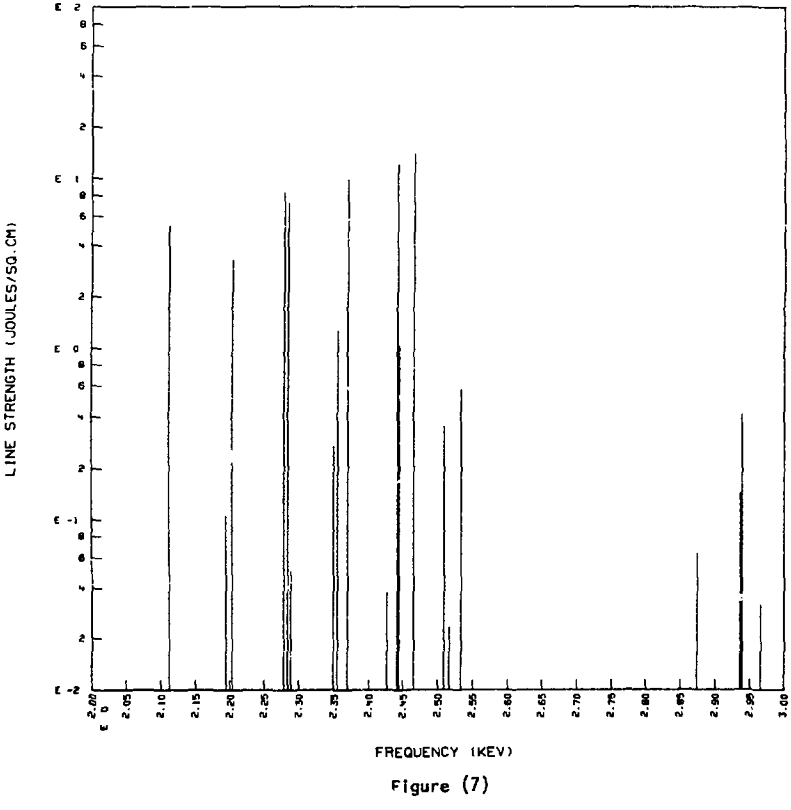
LINE STRENGTH (JOULES/SQ.CM)
E 2
8
6
4
2
E 1
8
6
4
2
E 0
8
6
4
2
E -1
8
6
4
2
E -2
2.00
E 0
2.05
2.10
2.15
2.20
2.25
2.30
2.35
2.40
2.45
2.50
2.55
2.60
2.65
2.70
2.75
2.80
2.85
2.90
2.95
3.00
FREQUENCY (KEV)

Figure (7)

(2-3) LINES OF ZIRCONIUM

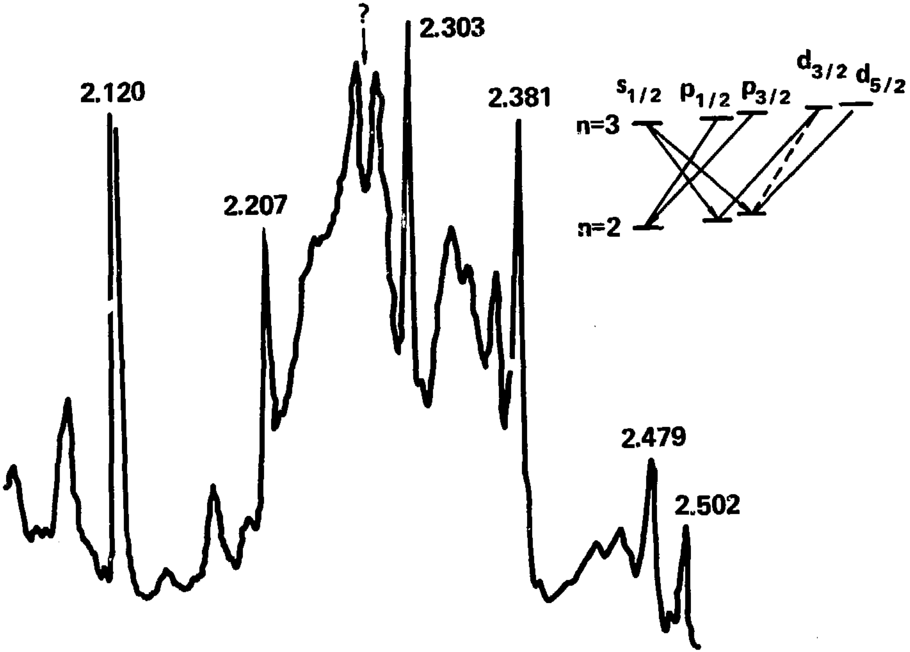

Figure (8)

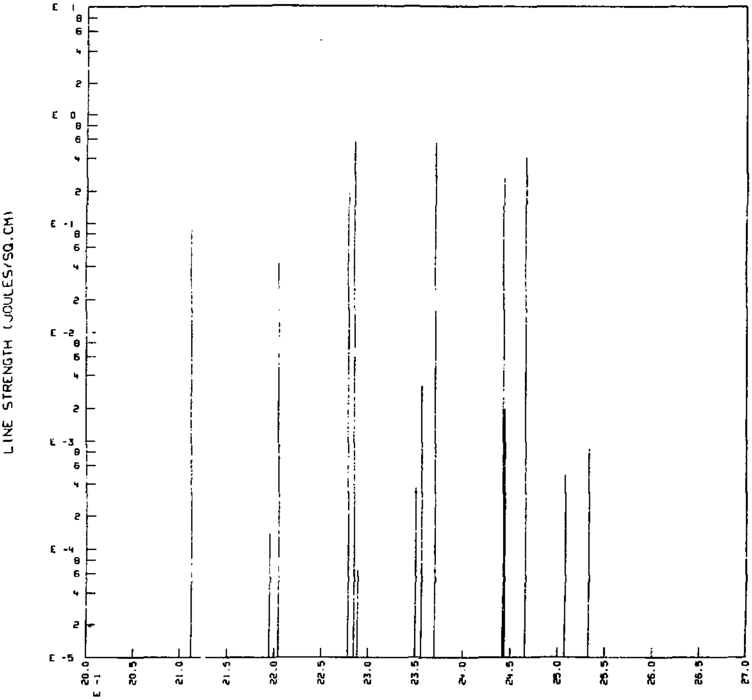
LINE STRENGTH (JOULES/SQ.CM)
E 1
8
6
4
2
E 0
8
6
4
2
E -1
8
6
4
2
E -2
8
6
4
2
E -3
8
6
4
2
E -4
8
6
4
2
E -5
20.0
E -1
20.5
21.0
21.5
22.0
22.5
23.0
23.5
24.0
24.5
25.0
25.5
26.0
26.5
27.0
FREQUENCY (KEV)

Figure (9)

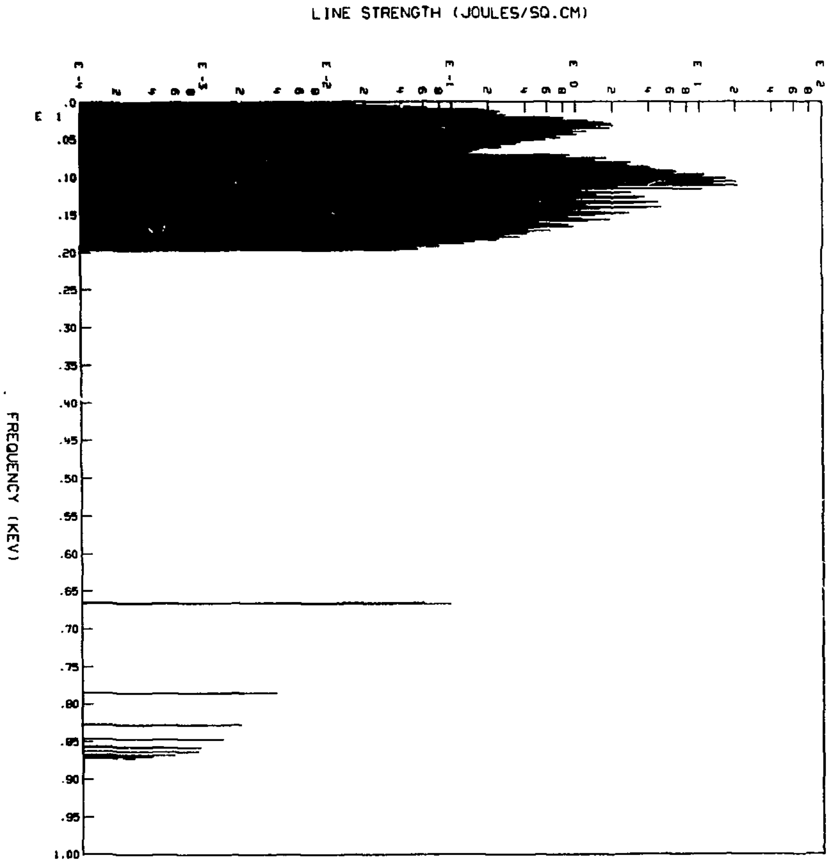
LINE STRENGTH (JOULES/SQ.CM)
E-4
2
4
6
8
E-3
2
4
6
8
E-2
2
4
6
8
E-1
2
4
6
8
E 0
2
4
6
8
E 1
2
4
6
8
E 2
E 1
.0
.05
.10
.15
.20
.25
.30
.35
.40
.45
.50
.55
.60
.65
.70
.75
.80
.85
.90
.95
1.00
FREQUENCY (KEV)

Figure (10)

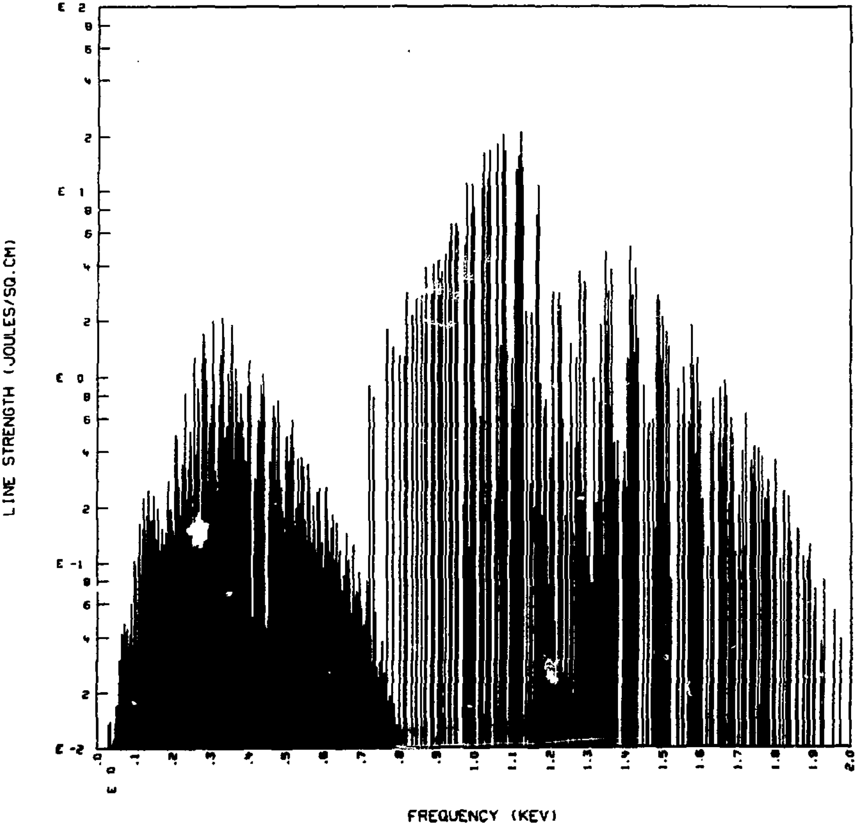
LINE STRENGTH (JOULES/SQ.CM)
E 2
8
6
4
2
E 1
8
6
4
2
E 0
8
6
4
2
E -1
8
6
4
2
E -2
.0
.1
.2
.3
.4
.5
.6
.7
.8
.9
1.0
1.1
1.2
1.3
1.4
1.5
1.6
1.7
1.8
1.9
2.0
E 0
FREQUENCY (KEV)

Figure (11)

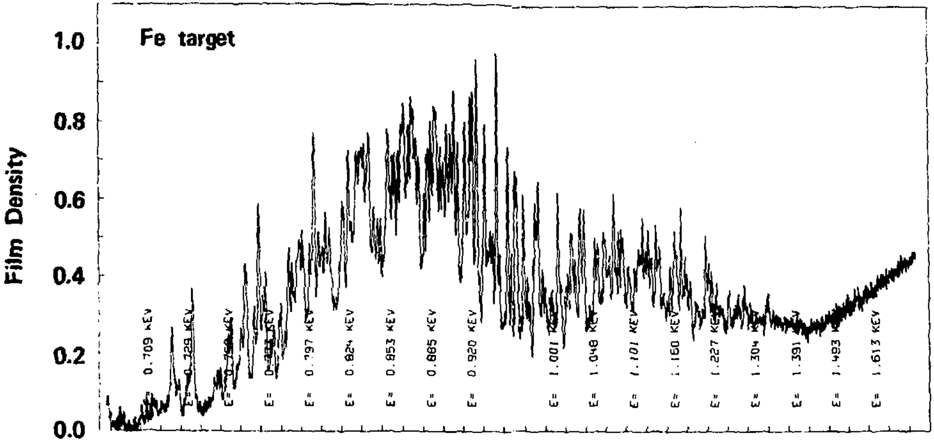
Film Density
1.0
0.8
0.6
0.4
0.2
0.0
Fe target
E= 0.709 KEV
E= 0.729 KEV
E= 0.750 KEV
E= 0.773 KEV
E= 0.797 KEV
E= 0.824 KEV
E= 0.853 KEV
E= 0.885 KEV
E= 0.920 KEV
E= 1.001 KEV
E= 1.048 KEV
E= 1.101 KEV
E= 1.160 KEV
E= 1.227 KEV
E= 1.304 KEV
E= 1.391 KEV
E= 1.493 KEV
E= 1.613 KEV

Figure (12)

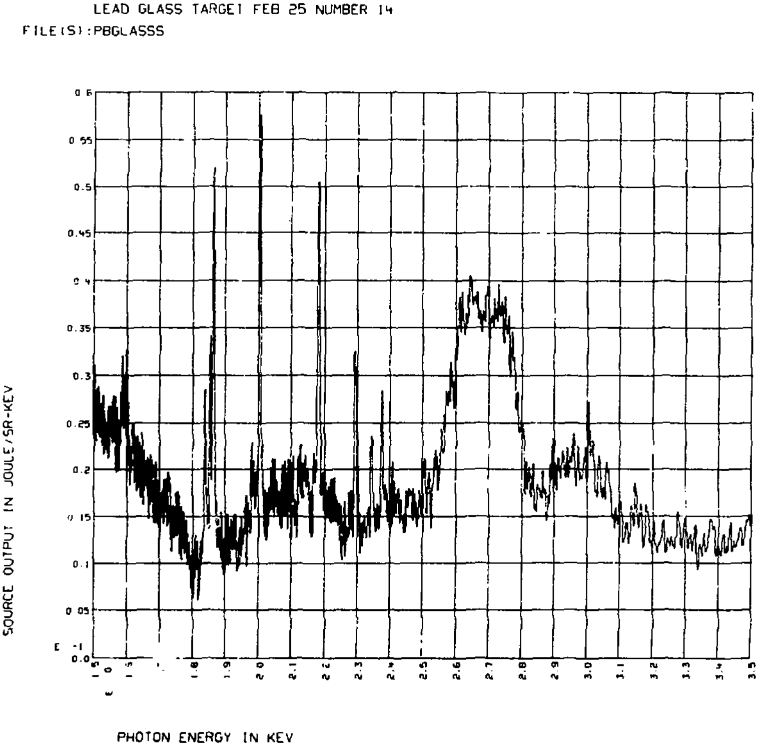
LEAD GLASS TARGET FEB 25 NUMBER 14
FILE(S):PBGLASSS
SOURCE OUTPUT IN JOULE/SR-KEV
0.6
0.55
0.5
0.45
0.4
0.35
0.3
0.25
0.2
0.15
0.1
0.05
0.0
1.8
1.9
2.0
2.1
2.2
2.3
2.4
2.5
2.6
2.7
2.8
2.9
3.0
3.1
3.2
3.3
3.4
3.5
PHOTON ENERGY IN KEV

Figure (13)

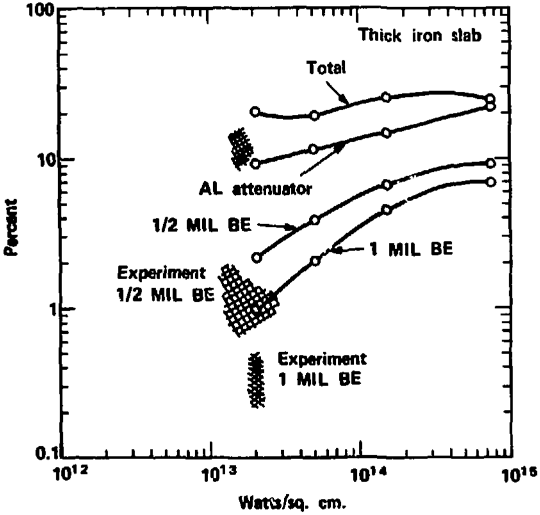

100
10
1
0.1
Percent
10^{12}
10^{13}
10^{14}
10^{15}
Watts/sq. cm.
Thick iron slab
Total
AL attenuator
1/2 MIL BE
1 MIL BE
Experiment
1/2 MIL BE
Experiment
1 MIL BE

Figure (14)

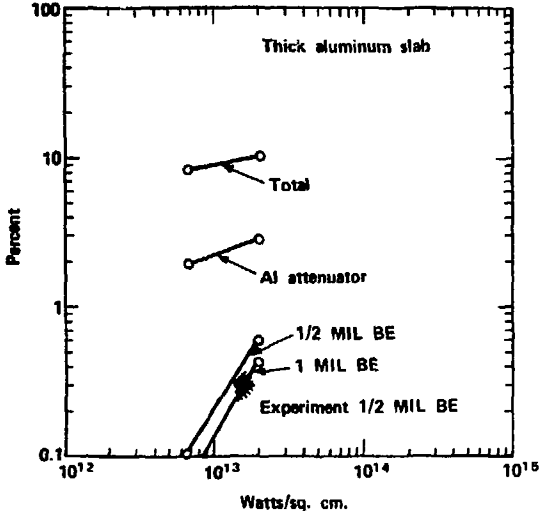
100
10
1
0.1
Percent
Thick aluminum slab
Total
Al attenuator
1/2 MIL BE
1 MIL BE
Experiment 1/2 MIL BE
10^{12}
10^{13}
10^{14}
10^{15}
Watts/sq. cm.

Figure (15)

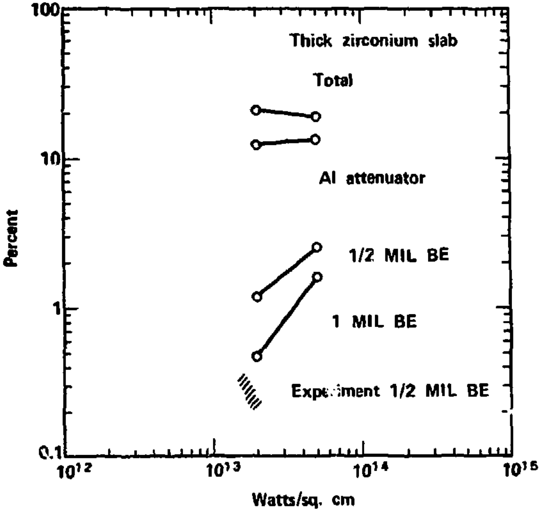
Thick zirconium slab
Total
Al attenuator
1/2 MIL BE
1 MIL BE
Experiment 1/2 MIL BE
Percent
100
10
1
0.1
10^{12}
10^{13}
10^{14}
10^{15}
Watts/sq. cm

Figure (16)

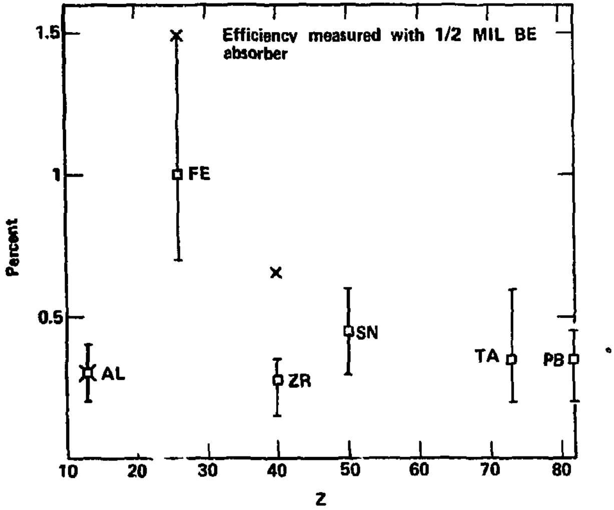
Efficiency measured with 1/2 MIL BE absorber
Percent
1.5
1
0.5
FE
AL
ZR
SN
TA
PB
10
20
30
40
50
60
70
80
Z

Figure (17)

DISTRIBTUION

W. H. Grasberger	40
TID File	15
TIC, Oak Ridge, TN	27

Printed in the United States of America
Available from
National Technical Information Service
U.S. Department of Commerce
5285 Port Royal Road
Springfield, Virginia 22151
Price: Printed Copy $____*; Microfiche $2.25

*Pages	NTIS Selling Price
1-50	$4.00
51-150	$5.45
151-325	$7.60
326-500	$10.60
501-1000	$13.60